

1                    **Likelihood based Mendelian randomization analysis with**  
2                    **automated instrument selection and horizontal pleiotropic modeling**

3

4    Zhongshang Yuan<sup>1,2</sup>, Lu Liu<sup>1,2</sup>, Ping Guo<sup>1,2</sup>, Ran Yan<sup>1,2</sup>, Fuzhong Xue<sup>1,2</sup>, Xiang  
5    Zhou<sup>3,4\*</sup>

6    <sup>1</sup> Department of Biostatistics, School of Public Health, Cheeloo College of Medicine,  
7    Shandong University, 250012 Jinan, Shandong, China;

8    <sup>2</sup> Institute for Medical Dataology, Cheeloo College of Medicine, Shandong University,  
9    250012 Jinan, Shandong, China;

10   <sup>3</sup> Department of Biostatistics, University of Michigan, Ann Arbor, MI 48109, USA;

11   <sup>4</sup> Center for Statistical Genetics, University of Michigan, Ann Arbor, MI 48109, USA

12   \*Corresponding author. Email: [xzhousph@umich.edu](mailto:xzhousph@umich.edu)

1 **Abstract**

2 Mendelian randomization (MR) is a common tool for identifying causal risk factors  
3 underlying diseases. Here, we present a method, MRAID, for effective MR analysis.  
4 MRAID borrows ideas from fine mapping analysis to model an initial set of candidate  
5 SNPs that are in potentially high linkage disequilibrium with each other and  
6 automatically selects among them the suitable instruments for causal inference.  
7 MRAID also explicitly models both uncorrelated and correlated horizontal pleiotropic  
8 effects that are widespread for complex trait analysis. MRAID achieves both tasks  
9 through a joint likelihood framework and relies on a scalable sampling-based algorithm  
10 to compute calibrated  $p$ -values. Comprehensive and realistic simulations show MRAID  
11 can provide calibrated type I error control, reduce false positives, while being more  
12 powerful than existing approaches. We illustrate the benefits of MRAID for an MR  
13 screening analysis across 645 trait pairs in UK Biobank, identifying multiple lifestyle  
14 causal risk factors of cardiovascular disease-related traits.

15

## 1 **Introduction**

2 Investigating causal relationship among complex traits and identifying causal risk  
3 factors are an important first step towards understanding the biology of diseases. A  
4 common statistical tool for performing such causal inference in observational studies is  
5 Mendelian randomization (MR). MR is a form of instrumental variable analysis that  
6 uses SNPs to serve as instruments for inferring the causal effect of an exposure variable  
7 on an outcome variable(1). MR requires only summary statistics from genome-wide  
8 association studies (GWASs) and is often performed in a two-sample study setting  
9 where the exposure variable and the outcome variable are measured in two separate  
10 studies(2). With the abundant availability of GWAS summary statistics, numerous MR  
11 analyses are being carried out, identifying important causal risk factors for various  
12 common diseases. These MR studies are facilitated by many recently developed MR  
13 methods that include the inverse variance weighted (IVW) method, MR-Egger(3),  
14 median-based regression(4), BWMR(5), RAPS(6), MRMix(7), CAUSE(8), to name a  
15 few. Different MR methods differ in their modeling assumptions and inference  
16 algorithms, but the majority of them encounter two important modeling and algorithmic  
17 challenges that have so far limited the effectiveness of MR analysis.

18 First, almost all existing MR methods rely on a pre-selected set of independent  
19 SNPs to serve as instruments for MR analysis. The instruments are selected to be  
20 independent from each other to ensure the validity of the statistical inference framework  
21 used in many common MR methods such as IVW. The independent SNPs are often  
22 selected through linkage disequilibrium (LD) clumping, a procedure that first ranks  
23 SNPs based on their marginal association evidence with the exposure variable and then  
24 retains SNPs that are not in high LD with the SNPs on top of the ranking list. Using LD  
25 clumping to select SNPs may be suboptimal, however, as the selected SNPs may only

1 represent tagging SNPs that are in LD with the causal SNPs rather than the causal ones  
2 themselves. Using tagging SNPs instead of the causal ones to serve as instruments can  
3 reduce the power of MR analysis. In addition, perhaps more importantly, selecting  
4 independent SNPs for MR analysis may not be ideal either, as complex traits can be  
5 influenced by multiple causal SNPs residing in the same local region that are in  
6 potential LD with each other. Consequently, selecting independent SNPs may only  
7 capture a small proportion of the phenotypic variance in the exposure variable, again  
8 leading to a loss of power in the subsequent MR analysis (1, 2, 9, 10). Indeed, in the  
9 parallel research field of transcriptome-wide association studies, it has been well  
10 documented that incorporating correlated SNPs can substantially improve analysis  
11 power than using independent SNPs only(11-14). Therefore, incorporating correlated  
12 SNPs and developing effective approaches to select instruments among them are  
13 important to fully captivate the potential of MR.

14 Second, only a limited number of MR methods model horizontal pleiotropy and  
15 even fewer can effectively control for it during MR analysis(15). Horizontal pleiotropy  
16 occurs when the SNP instruments exhibit effects on the outcome through pathways  
17 other than the exposure. Horizontal pleiotropy has been widely observed in complex  
18 trait analysis(13, 15) and often comes in two distinct types. The first type of horizontal  
19 pleiotropy arises through paths independent of the exposure, with the resulting  
20 horizontal pleiotropic effects being independent of the SNP effects on the exposure. The  
21 second type of horizontal pleiotropy arises through unobserved exposure-outcome  
22 confounders and induces correlation between the horizontal pleiotropic effects and the  
23 SNP effects on the exposure. The presence of either type of horizontal pleiotropy  
24 violates standard MR modeling assumptions and can lead to biased causal effect  
25 estimates and increased false discoveries. Early MR analyses control for horizontal

1 pleiotropy by simply removing instrumental SNPs that are potentially associated with  
2 the outcome variable(15-18). Removing SNPs associated with the outcome would  
3 result in a conservative set of selected instruments and lead to a loss of power in the  
4 subsequent MR analysis. Recent MR methods explicitly model horizontal pleiotropy  
5 by specifying modeling assumptions on the horizontal pleiotropic effects. For example,  
6 the Egger assumption assumes the same horizontal pleiotropic effect across SNP  
7 instruments(3, 13), while PMR-VC(13) and BWMR(5) assume the horizontal  
8 pleiotropic effects to follow a normal distribution; all these methods model the first type  
9 of horizontal pleiotropy. MRMix(7) and CAUSE(8), by contrast, employ a normal-  
10 mixture model to control for both types of horizontal pleiotropy. Unfortunately,  
11 modeling both types of horizontal pleiotropy has been technically challenging, as the  
12 resulting likelihood function of the MR model often consists of an integration that  
13 cannot be solved analytically. Consequently, both MRMix and CAUSE rely on non-  
14 likelihood based approaches to perform MR inference. Specifically, MRMix searches  
15 on a grid of causal effect candidates to identify the one that maximizes the proportion  
16 of GWAS summary statistics residing in the expected sub-model without horizontal  
17 pleiotropy. CAUSE contrasts the out-of-sample prediction accuracy between two  
18 different models, one with the causal effect and the other without, by computing the  
19 expected log pointwise posterior density between the two, for causal inference. Non-  
20 likelihood based causal inference, however, can lead to a loss of power and/or  
21 uncalibrated test statistics that are essential for large-scale screening of causal risk  
22 factors underlying diseases. Indeed, as we will show here, MRMix is not robust to  
23 modeling misspecifications on the instrumental effect sizes and is prone to estimation  
24 bias, while CAUSE yields overly conservative  $p$ -values.

1           Here, we present a likelihood-based two-sample MR method for causal inference  
2 that overcomes the above two challenges. Specifically, our method models an initial set  
3 of candidate SNP instruments that are in high LD with each other and automatically  
4 selects among them the suitable instruments for MR analysis. In addition, our method  
5 accounts for both types of horizontal pleiotropy in a likelihood framework and relies  
6 on a scalable sampling-based algorithm for calibrated  $p$ -values computation. We refer  
7 to our method as the two-sample Mendelian Randomization with Automated  
8 Instrument Determination (MRAID). We demonstrate the effectiveness of MRAID  
9 through comprehensive and realistic simulations. We also apply MRAID for an MR  
10 screening analysis across 645 trait pairs in the UK Biobank(19), identifying lifestyle  
11 risk factors that may causally influence cardiovascular disease-related traits.

12

## 1 **Results**

### 2 **Method overview**

3 MRAID is described in the [Materials and Methods](#), with its technical details provided  
4 in the [Supplementary Text](#) and a method schematic shown in [Fig. 1](#). Briefly, MRAID  
5 is a two-sample MR method that aims to infer the causal effect of an exposure variable  
6 on an outcome variable using GWAS summary statistics. MRAID models jointly all  
7 genome-wide significant SNPs that are in potential LD with each other and performs  
8 automated instrument selection among them to identify suitable instruments for MR  
9 analysis. In addition, MRAID explicitly accounts for two types of horizontal pleiotropic  
10 effects through a maximum likelihood-based inference framework and is scalable to  
11 biobank datasets ([Table 1](#)).

12

### 13 **Simulations: Type I error control**

14 We evaluated the performance of MRAID and compared it with six existing MR  
15 methods in simulations (details in [Materials and Methods](#)). We first examined type I  
16 error control of different methods in different scenarios. In the absence of both  
17 correlated and uncorrelated horizontal pleiotropic effects, most methods, including  
18 MRAID, IVW-R, Robust, RAPS and MRMix, all yield reasonably calibrated type I  
19 error control ([Fig. 2A](#)). Weighted mode and CAUSE, on the other hand, display overly  
20 conservative type I error control, which is consistent with the original studies(7, 8, 20).  
21 The null  $p$ -value distributions from different methods remain largely similar regardless  
22 of the number of SNPs that affect the exposure ([Fig. S1A](#)) and their total effects on the  
23 exposure ([Fig. S1B](#)). We further examined the robustness of different methods in  
24 settings where the SNP effects on the exposure do not follow a simple normal  
25 distribution but with some SNPs displaying larger effects than the others. In these

1 settings, MRAID, IVW-R and RAPS remain calibrated, while both MRMix and Robust  
2 method show inflated type I errors, presumably due to their restricted normality  
3 assumptions on the SNP effect sizes (Fig. 2B). Note that we directly used correlated  
4 SNPs for MRAID but performed clumping to select independent SNPs for the other  
5 methods. Without clumping, all other MR methods produce overly inflated type I errors  
6 (Fig. S2).

7 We examined the effects of horizontal pleiotropy on type I error control for different  
8 methods. When horizontal pleiotropic effects are present but are uncorrelated with the  
9 instrumental effects, MRAID maintains type I error control (Fig. 2C). In contrast, both  
10 Weighted mode and CAUSE remain overly conservative, while MRMix, Robust, IVW-  
11 R and RAPS yield inflated  $p$ -values (Fig. 2C). Similar conclusion holds regardless of  
12 the effect size for the uncorrelated horizontal pleiotropy or the proportion of SNPs that  
13 display uncorrelated pleiotropic effects (Fig. S3). The  $p$ -value inflation problem of  
14 MRMix relieves when the proportion of SNPs that display uncorrelated horizontal  
15 pleiotropic effects decreases. When correlated horizontal pleiotropic effects are also  
16 present in addition to the uncorrelated horizontal pleiotropic effects, MRAID maintains  
17 effective type I error control (Fig. 2D). In contrast, both Weighted mode and CAUSE  
18 remain overly conservative, while MRMix, Robust, IVW-R and RAPS produce inflated  
19  $p$ -values. Similar conclusion holds regardless of the effect size of the correlated  
20 horizontal pleiotropy (Fig. S4A vs Fig. S4C), the proportion of SNPs that display  
21 uncorrelated horizontal pleiotropic effects (Fig. S4A vs Fig. S4B), the proportion of  
22 SNPs that display correlated horizontal pleiotropic effects (Fig. S4A vs Fig. S4D), or  
23 how the correlated horizontal pleiotropic effects are created (Fig. S5).

24

25 **Simulations: Power comparison**



1 We examined the power of different MR methods to detect non-zero causal effect.  
2 Because the same  $p$ -value from different methods may correspond to different type I  
3 errors, we computed power based on an false discovery rate (FDR) of 0.05 instead of a  
4 nominal  $p$ -value threshold to allow for fair comparison among methods. In the absence  
5 of both uncorrelated and correlated horizontal pleiotropic effects, MRAID, IVW-R and  
6 RAPS all have higher power than the other methods across different scenarios. Among  
7 these three methods, MRAID is slightly more powerful than the other two when the  
8 instrumental effects are small or when the causal effect is small (Fig. 3A, 3B),  
9 presumably due to the automated instrument selection procedure employed in MRAID.  
10 MRAID is slightly less powerful than the other two when the instrumental effects are  
11 large and the causal effect is large (Fig. S6), as the simple instrumental selection  
12 approaches used in the other methods can be effective in these lesser challenging  
13 settings. The performance of these three methods is generally followed by Robust.  
14 While Weighted mode, MRMix, and, to a lesser extent, CAUSE, have low power.

15 We examined the influence of horizontal pleiotropy on the power of different  
16 methods. When horizontal pleiotropic effects are present but are uncorrelated with the  
17 instrumental effects, MRAID is more powerful than the other MR methods (Fig. 3C).  
18 The power gain brought by MRAID becomes more apparent with increasing horizontal  
19 pleiotropy, which is characterized by increased horizontal pleiotropic effect sizes  
20 and/or increased proportion of SNPs that display horizontal pleiotropic effects (Fig. S7).  
21 The performance of MRAID is often followed by RAPS, Robust, CAUSE, and IVW-  
22 R, while MRMix and Weighted mode generally have low power (Fig. S7). Among these  
23 methods, the performance of IVW-R is particularly sensitive to the horizontal  
24 pleiotropic effect sizes or the proportion of SNPs that display horizontal pleiotropic  
25 effects. When correlated horizontal pleiotropic effects are also present in addition to the

1 uncorrelated horizontal pleiotropic effects, the power of MRAID remains higher than  
2 the other methods. The higher power of MRAID maintains regardless of the correlated  
3 horizontal pleiotropic effect sizes, the proportion of instrumental SNPs that display  
4 correlated horizontal pleiotropic effects (Fig. 3D, Fig. S7D-F), or how the correlated  
5 horizontal pleiotropic effects are created (Fig. S8). The power gain brought by MRAID  
6 is particularly apparent with increased proportion of instrumental SNPs that display  
7 uncorrelated horizontal pleiotropic effects (Fig. 3D vs Fig. S7F, Fig. S7E vs Fig. S7D).  
8 Importantly, the power of MRAID is close to an oracle MR approach that uses the  
9 actual set of instrumental SNPs for MR inference, especially when the casual effect size  
10 is large, supporting the effectiveness of the automatic instrument selection procedure  
11 in MRAID (Fig. S9).

12 Next, we examined the ability of different MR methods in distinguishing the causal  
13 effect direction through reverse causality analysis. In particular, we tested the causal  
14 effect of the outcome on the exposure in the alternative simulations where the exposure  
15 had casual effect on the outcome but not vice versa. In the presence of horizontal  
16 pleiotropy, the SNP instruments obtained for the outcome in the reverse MR analysis  
17 would contain two sets of SNPs: a set of exposure SNP instruments that are indirectly  
18 associated with the outcome through the exposure and a set of SNPs that are directly  
19 associated with the outcome through their horizontal pleiotropic effects on the outcome.  
20 Because the two sets of SNPs displayed heterogeneous effects on the exposure, we  
21 would fail to detect a non-zero causal effect of the outcome on the exposure. Therefore,  
22 the reverse causality analysis in the presence of horizontal pleiotropy effectively served  
23 as analysis on null simulations. Indeed, we found that MRAID provides effective type  
24 I error control and calibrated  $p$ -values in the reverse causality analysis across a range  
25 of simulation scenarios (Fig. S10 and S11). In contrast, the type I error control of the

1 other methods is highly dependent on the extent of the horizontal pleiotropy.  
2 Specifically, when a small proportion of exposure instrumental SNPs display horizontal  
3 pleiotropy on the outcome, the majority of the candidate instrumental SNPs for the  
4 outcome in the reverse causality analysis would not display horizontal pleiotropic  
5 effects on the exposure. In this case, both CAUSE and Weighted mode remain overly  
6 conservative, while IVW-R, MRMix, RAPS and Robust yield slightly inflated  $p$ -values  
7 (Fig. S10A, S10C, S11A, and S11C). By contrast, when a large proportion of  
8 instrumental SNPs for the exposure display horizontal pleiotropic effects on the  
9 outcome, the majority of the candidate instrumental SNPs for the outcome in the reverse  
10 causality analysis would display horizontal pleiotropic effects on the exposure. In this  
11 case, MRMix, Robust, IVW-R and RAPS all start to produce inflated  $p$ -values (Fig.  
12 S10B and S11B) as we have shown in the corresponding null scenarios. The  $p$ -value  
13 information of these methods becomes more prominent with smaller horizontal  
14 pleiotropic effect sizes, where it becomes increasingly hard to select the second set of  
15 SNPs to serve as outcome instruments (Fig. S10D and S11D).

16 Finally, MRAID produces reasonably unbiased causal effect estimates under the  
17 null (Fig. S12A) and under various alternatives (Fig. S12B-D).

18

## 19 **Real data applications**

20 We applied MRAID and the other MR methods to analyze 38 lifestyle risk factors and  
21 11 CVD-related traits in the UK Biobank (details in [Materials and Methods](#)).  
22 Specifically, we divided the UK Biobank data into two separate, equal-sized subsets,  
23 representing an exposure GWAS and an outcome GWAS. We performed two sets of  
24 analysis. First, we focused on the eight CVD-related traits and examined the causal  
25 effect of each trait in the exposure GWAS on the same trait in the outcome GWAS,

1 effectively examining the causal effect of the trait on itself. The true causal effect in  
2 such analysis is non-zero and equals exactly one. In the analyses, we found that all  
3 methods were able to detect a non-zero causal effect for the trait on itself across all  
4 eight CVD-related traits (Fig. 4). However, only MRAID and CAUSE were able to  
5 produce 95% confidence intervals that cover the true causal effects for all eight trait  
6 pairs, with CAUSE producing confidence intervals that are 2.39-5.69 times larger than  
7 MRAID (Fig. 4). For example, in the HDL-HDL analysis, MRAID (estimate = 0.98;  
8 95% CI: 0.96-1.01), CAUSE (0.95; 0.82-1.09) and MRMix (0.96; 0.90-1.02) correctly  
9 inferred the causal effect, with MRAID providing the smallest confidence interval (Fig.  
10 4H). In contrast, the confidence intervals from the other four methods did not cover the  
11 true causal effect of one. In the LDL-LDL analysis, MRAID (0.97; 0.94-1.01) and  
12 CAUSE (0.96; 0.84-1.08) correctly inferred the causal effect, with MRAID providing  
13 a smaller confidence interval (Fig. 4F). While the confidence intervals from the other  
14 five methods also did not cover the true causal effect of one. The results suggest that  
15 both MRAID and CAUSE can produce accurate causal effect estimates and calibrated  
16 confidence intervals for trait on itself analysis, with MRAID being more powerful than  
17 CAUSE.

18 Next, we investigated the causal relationship between 38 lifestyle risk factors and  
19 11 CVD-related traits. The association of lifestyle risk factors on CVD-related traits  
20 has been extensively documented(21, 22). However, it remains controversial on  
21 whether the detected associations are causal as some of the association effects were  
22 estimated to have different signs in different studies(23, 24). We performed both  
23 forward causality analysis examining the causal effects of lifestyle factors on CVD-  
24 related traits and reverse causality analysis examining the causal effects of CVD-related  
25 traits on lifestyle factors. The distribution of  $p$ -values for the analyzed trait pairs from

1 different methods are shown in Fig. 5A. Consistent with the simulations, we found that  
2 the  $p$ -values from MRAID (genomic inflation factor, GIF =0.90), and to a lesser extent  
3 MRMix (GIF = 0.78), are generally well behaved and slightly conservative across  
4 analyzed trait pairs, more so than the other methods (Fig. 5A). Also consistent with the  
5 simulations, we found that the  $p$ -values from CAUSE are overly conservative (GIF =  
6 0.12), while the  $p$ -values from RAPS (GIF = 1.96), Weighted mode (GIF = 1.70), IVW-  
7 R (GIF = 2.12), and Robust (GIF = 2.00) all show appreciable inflation (Fig. 5A).  
8 Indeed, only MRAID produces calibrated  $p$ -values in the permutation analysis where  
9 we permuted the outcome trait (Fig. 5B).

10 Based on a Bonferroni corrected  $p$ -value threshold ( $8 \times 10^{-5}$ ), MRAID detected  
11 eight causal associations (Table S1), all of which have strong biological support. For  
12 example, MRAID detected a negative causal effect of smoking on BMI. The negative  
13 association between smoking and obesity has been well documented in observational  
14 studies(25, 26) and MR studies(27). Specifically, nicotine intake during smoking  
15 decreases resting metabolic rate(28, 29) and inhibits lipoprotein lipase activity and  
16 other kinase pathways to reduce lipolysis(26), all of which lead to a reduction in the net  
17 energy storage in adipose tissues and subsequent weight loss(30). Nicotine also  
18 activates acetylcholine receptors in the hypothalamus and subsequently anorexigenic  
19 neurons(31, 32), which leads to suppressed appetite and food intake. As another  
20 example, MRAID detected an effect of age started smoking in the former smokers on  
21 HDL, suggesting a negative effect of smoking behavior on HDL. Smoking behavior in  
22 general is well known to be causally associated with HDL(33). In particular, smoking  
23 can modify the activity of critical enzymes for lipid transport, lower lecithin-cholesterol  
24 acyltransferase (LCAT) activity, and alter cholesterol ester transfer protein (CETP) and  
25 hepatic lipase activity, all of which can reduce HDL metabolism. In addition, smoking

1 induces oxidative modifications that render HDL dysfunctional and deprive its  
2 atheroprotective properties(34, 35).

3       Importantly, MRAID did not mistakenly detect many false causal associations that  
4 were detected by the other methods. A well-known example of a potential false causal  
5 association is the effect of smoking on blood pressure. A negative association between  
6 smoking and blood pressure has been observed in observational studies(22). However,  
7 multiple subsequent MR studies on large datasets did not support a causal relationship  
8 between the two traits(33, 36). Indeed, the association between smoking and blood  
9 pressure in observational studies is likely confounded by factors that include, but not  
10 limited to age, BMI, social class, salt intake, drinking habits, as well as unmeasured  
11 confounders(37). Consistent with these previous MR studies, MRAID did not detect a  
12 significant causal effect from any of the eight smoking related traits on either SBP or  
13 DBP. In contrast, almost all other methods falsely detected causal effects of some of  
14 the smoking related traits on blood pressure. For example, the causal effect of the  
15 number of unsuccessful stop-smoking attempts on SBP is not detected by MRAID ( $p =$   
16  $0.44$ ), CAUSE ( $p = 0.01$ ) nor Weighted mode ( $p = 1.3 \times 10^{-4}$ ), but falsely identified  
17 by IVW-R ( $p = 1.4 \times 10^{-6}$ ), Robust ( $p = 4.1 \times 10^{-34}$ ), RAPS ( $p = 5.5 \times 10^{-6}$ ), and  
18 MRMix ( $p = 2.8 \times 10^{-6}$ ). Similarly, the causal effect of age started smoking in former  
19 smokers on SBP is not detected by MRAID ( $p = 0.06$ ) nor CAUSE ( $p = 1.3 \times 10^{-3}$ ),  
20 but falsely detected by IVW-R ( $p = 7.8 \times 10^{-5}$ ), Robust ( $p = 1.5 \times 10^{-30}$ ), RAPS  
21 ( $p = 8.9 \times 10^{-7}$ ), Weighted mode ( $p = 1.7 \times 10^{-6}$ ), and MRMix ( $p = 4.1 \times 10^{-7}$ ).  
22 As another false example, BMI is unlikely to causally influence the time spent driving,  
23 at least not positively. Indeed, MRAID ( $p = 0.01$ ), along with MRMix ( $p = 0.12$ ),  
24 CAUSE ( $p = 0.02$ ) and Weighted mode ( $p = 0.04$ ), did not detect any causal effect of

1 BMI on time spent driving. However, both IVW-R ( $p = 2.5 \times 10^{-6}$ ) and RAPS ( $p =$   
2  $3.1 \times 10^{-5}$ ) detected a false positive effect of BMI on time spent driving.

3 Finally, we note that an important feature of MRAID is its ability to effectively  
4 decompose the SNP effects on the outcome into three distinct paths: one directly acts  
5 from SNPs to the outcome, one mediated through the exposure, and the other acts  
6 through a hidden confounding factor that influences both exposure and outcome.  
7 Consequently, MRAID can be used to estimate the proportion of SNPs in different  
8 categories, including the proportion of SNPs that are associated with the exposure  
9 among the genome-wide significant ones ( $\pi_\beta$ ), the proportion of SNPs that exhibit  
10 correlated horizontal pleiotropy ( $\pi_c$ ), the proportion of SNPs that exhibit uncorrelated  
11 horizontal pleiotropy among the selected instruments ( $\pi_1$ ), and the proportion of SNPs  
12 that exhibit uncorrelated horizontal pleiotropy among the remaining candidate  
13 instruments ( $\pi_0$ ). In the real data applications, we estimated the mean of  $\pi_\beta$ ,  $\pi_c$ ,  $\pi_1$   
14 and  $\pi_0$  across the 645 analyzed trait pairs to be 14.6%, 6.4%, 16.4%, and 5%,  
15 respectively (Fig. S13). In addition, we estimated their means in the eight significant  
16 trait pairs to be 6.2%, 5.7%, 11.4%, and 0.1%, respectively. The proportion of SNPs  
17 displaying correlated pleiotropy is also highly correlated with the proportion of SNPs  
18 displaying uncorrelated pleiotropy, with the latter generally being larger than the former  
19 (Fig. S14). These proportion estimates support the wide-spread horizontal pleiotropy  
20 previously identified in complex trait analysis(15) and provide detailed quantifications  
21 on the extent to which the two types of horizontal pleiotropy influence MR analysis.

22

## 1 **Discussion**

2 We have presented MRAID, a two-sample MR method that can automatically select  
3 suitable instruments from a candidate set of correlated SNPs and that can control for  
4 both correlated and uncorrelated horizontal pleiotropy in a likelihood-based inference  
5 framework. Overall, by automatically selecting instrumental SNPs and performing  
6 inference under a likelihood-based framework, MRAID yields calibrated  $p$ -values  
7 across a wide range of scenarios and improves power of MR analysis over existing  
8 approaches. We have illustrated the benefits of MRAID through simulations and  
9 applications to complex trait analysis.

10 We have primarily focused on modeling quantitative traits with MRAID in the  
11 present study. For binary exposures and outcomes, one could treat them as continuous  
12 variables and directly applied MRAID for MR analysis. Treating binary exposures and  
13 outcomes as continuous variables can be justified by recognizing the linear model as a  
14 first-order Taylor approximation to a generalized linear model such as the logistic  
15 regression(38). However, such approximation is accurate only when the SNP effects on  
16 the exposure and outcome are relatively small. While similar approaches have been  
17 applied in many previous MR studies(39-41), we caution that the interpretation of the  
18 causal effect estimate can be challenging when the linear models are used to fit binary  
19 exposures and outcomes, especially when a two-stage inference procedure is used for  
20 MR analysis(42, 43). For example, when a binary exposure is a dichotomization of a  
21 continuous risk factor, the causal effect estimation through modeling the binary  
22 exposure without the underlying continuous risk factor may require additional  
23 modeling assumptions, even when the main MR assumptions are satisfied. In addition,  
24 modeling binary exposure without the underlying continuous risk factor can lead to  
25 violation of the exclusion restriction assumption, as the instruments can influence the



1 outcome via the continuous risk factor even if the binary exposure does not change.  
2 Therefore, extending MRAID to explicitly model data types beyond quantitative traits  
3 is important to ensure its wide applicability. Because MRAID builds upon a data  
4 generative model and performs inference on the SNP-exposure model and the SNP-  
5 outcome model jointly through a maximum likelihood-based framework, it can be  
6 naturally extended towards modeling other types of exposure or outcome data, through,  
7 for example, a generalized linear model framework. To the best of our knowledge, the  
8 only likelihood-based MR method that accommodates both binary risk factors and  
9 outcome is IV-MVB(44). IV-MVB, however, requires individual-level data, applies to  
10 the one-sample analysis setting, and cannot easily handle multiple instruments in a  
11 computationally efficient fashion especially for those that are correlated. Therefore,  
12 exploring the benefits of MRAID extensions towards modeling generalized data types  
13 while keeping computation in check will be an important direction for future research.

14 MRAID is not without limitations. First, while MRAID performs automated  
15 selection on SNP instruments, such selection builds upon a sparsity inducing modeling  
16 assumption specified on the SNP effect sizes. The sparse modeling assumption contains  
17 multiple hyper-parameters that rely on a sampling-based algorithm for inference.  
18 Accurate and robust inference of the hyper-parameters will likely require at least a  
19 moderate number of candidate instruments. While the significance of the trait pairs  
20 evaluated by MRAID in our real data application does not appear to be dependent on  
21 the number of candidate instruments selected for the trait pair (Fig. S15), we caution  
22 that MRAID may incur low power when the instrumental effect size is small and the  
23 number of candidate instruments is low, which can happen in GWAS with small sample  
24 sizes and for exposure traits with a non-polygenic architecture. Second, MRAID  
25 primarily follows the approach of CAUSE to model correlated horizontal pleiotropy by

1 introducing a single latent variable to serve as the confounder for both the exposure and  
2 the outcome. Because of its limitation in modeling only a single unobserved  
3 confounding factor, MRAID may not be fully effective in settings where multiple or  
4 other types of shared genetic components are present between the exposure and the  
5 outcome. Finally, the summary statistics version of MRAID requires as input two LD  
6 matrices, one from the exposure GWAS and another from the outcome GWAS. In the  
7 present study, we have estimated both LD matrices using individual level data. In the  
8 absence of individual level data, both LD matrices may be estimated from a reference  
9 panel with the same genetic ancestry (e.g. from the 1,000 Genomes Project). However,  
10 care needs to be taken when the exposure and outcome GWASs are carried out on two  
11 populations with distinct genetic ancestries.  
12

## 1 **Materials and Methods**

### 2 **MRAID for individual level data**

3 We provide an overview of our method here, with its inference and technical details  
4 provided in the [Supplementary Text](#) and an illustrative diagram displayed in [Fig. 1](#). Our  
5 goal is to estimate and test the causal effect of an exposure variable on an outcome  
6 variable in the two-sample MR setting where the exposure and outcome variables are  
7 measured in two separate GWASs with no sample overlap. We refer to the two separate  
8 GWASs as the exposure GWAS and the outcome GWAS, respectively. To set up the  
9 notations, we denote  $\mathbf{x}$  as an  $n_1$ -vector of the exposure variable measured on  $n_1$   
10 individuals in the exposure GWAS. We denote  $\mathbf{y}$  as an  $n_2$ -vector of the outcome  
11 variable measured on  $n_2$  individuals in the outcome GWAS. We scale both  $\mathbf{x}$  and  $\mathbf{y}$   
12 to have zero mean and unit standard deviation. In the exposure GWAS, we perform an  
13 initial screening to select SNPs that are associated with the exposure variable with a  
14 marginal  $p$ -value below the genome-wide significance threshold of  $5 \times 10^{-8}$ . These  
15 SNPs are likely in LD with each other and are selected to serve as the initial set of  
16 candidate instruments. We denote  $\mathbf{Z}_x$  as the resulting  $n_1$  by  $p$  genotype matrix for the  
17  $p$  selected candidate instrumental SNPs in the exposure GWAS. We also denote  $\mathbf{Z}_y$  as  
18 an  $n_2$  by  $p$  genotype matrix for the same  $p$  candidate instrumental SNPs in the  
19 outcome GWAS. We scale each column of the two genotype matrices to have mean  
20 zero and standard deviation of one. We model the relationship among the exposure,  
21 outcome and genotypes through the following three linear regressions:

$$22 \quad \mathbf{x} = \mathbf{Z}_x \boldsymbol{\beta} + \boldsymbol{\varepsilon}_x, \quad (1)$$

$$23 \quad \tilde{\mathbf{x}} = \mathbf{Z}_y \boldsymbol{\beta} + \tilde{\boldsymbol{\varepsilon}}_x, \quad (2)$$

$$24 \quad \mathbf{y} = \tilde{\mathbf{x}} \boldsymbol{\alpha} + \mathbf{Z}_y \boldsymbol{\eta}_0 + \mathbf{Z}_y \boldsymbol{\eta}_1 + \boldsymbol{\varepsilon}_y. \quad (3)$$

1 Above, equation (1) describes the relationship between the genotypes  $\mathbf{Z}_x$  and the  
2 exposure variable  $\mathbf{x}$  in the exposure GWAS; equation (2) describes the relationship  
3 between the genotypes  $\mathbf{Z}_y$  and the unobserved exposure  $\tilde{\mathbf{x}}$  in the outcome GWAS;  
4 equation (3) describes the relationship among the genotypes  $\mathbf{Z}_y$ , the outcome  $\mathbf{y}$ , and  
5 the unobserved exposure  $\tilde{\mathbf{x}}$  in the outcome GWAS;  $\boldsymbol{\beta}$  is a  $p$ -vector of SNP effects on  
6 the exposure; both  $\boldsymbol{\eta}_0$  and  $\boldsymbol{\eta}_1$  are  $p$ -vectors of horizontal pleiotropy effects on the  
7 outcome;  $\alpha$  is a scalar that represents the causal effect of the exposure on the outcome;  
8  $\boldsymbol{\epsilon}_x$  is an  $n_1$ -vector of residual error with each element independently and identically  
9 distributed from a normal distribution  $N(0, \sigma_x^2)$ ;  $\tilde{\boldsymbol{\epsilon}}_x$  is an  $n_2$ -vector of residual error  
10 with each element distributed from the same normal distribution  $N(0, \sigma_x^2)$ ; and  $\boldsymbol{\epsilon}_y$  is  
11 an  $n_2$ -vector of residual error with each element distributed from a normal distribution  
12  $N(0, \sigma_y^2)$ . We note that while the above three equations are specified based on two  
13 separate GWASs, they are connected to each other by the common parameter  $\boldsymbol{\beta}$ . We  
14 carefully consider the modeling assumptions on the SNP effects on the exposure  
15 variable  $\boldsymbol{\beta}$  as well as the horizontal pleiotropic effects  $\boldsymbol{\eta}_0$  and  $\boldsymbol{\eta}_1$  as follows.

16 The  $p$  SNPs included in the above model represent an initial set of candidate  
17 instruments. While all the candidate instruments are marginally associated with the  
18 exposure, the majority of them are unlikely the causal SNPs for the exposure variable.  
19 Instead, most candidate instruments likely represent tagging SNPs that are associated  
20 with the exposure variable due to LD with the truly causal ones underlying the exposure.  
21 Therefore, it would be beneficial to perform additional selections on the candidate  
22 instruments to identify SNPs that are causal for the exposure and treat them as the  
23 instruments in order to maximize the power of MR analysis. To do so, we borrow ideas  
24 from fine-mapping approaches developed in the research field of GWAS and specify a  
25 sparsity inducing modeling assumption on the SNP effects on the exposure ( $\boldsymbol{\beta}$ ) to

1 perform automated instrument selection. In particular, we assume that  $\beta_j \sim \pi_\beta N(0,$   
2  $\sigma_\beta^2) + (1 - \pi_\beta)\delta_0$ , where  $\delta_0$  is the Dirac function that represents a point mass at zero.  
3 That is, with probability  $1 - \pi_\beta$ , the  $j$ -th SNP has zero effect on the exposure; while  
4 with probability  $\pi_\beta$ , the  $j$ -th SNP has a non-zero effect on the exposure and its effect  
5 size follows a normal distribution with mean zero and variance  $\sigma_\beta^2$ , where the variance  
6 parameter  $\sigma_\beta^2$  determines the magnitude of the effect sizes. The sparse assumption on  
7  $\beta$  allows us to select SNPs with non-zero effects on the exposure to serve as the  
8 instruments in the MR model.

9 In addition, the  $p$  SNPs included in the above model can also exhibit horizontal  
10 pleiotropic effects and influence the outcome variable through pathways other than the  
11 exposure. To control for the potential horizontal pleiotropic effects and improve causal  
12 effect inference, we introduce two sets of parameters,  $\eta_0$  and  $\eta_1$ , to model horizontal  
13 pleiotropic effects. The two sets of parameters are placed separately for the two SNP  
14 groups – the group of selected instrumental SNPs and the group of unselected non-  
15 instrumental SNPs – that are categorized by the sparse modeling assumption on  $\beta$ . In  
16 particular,  $\eta_1$  represents the horizontal pleiotropic effects exhibited by the selected  
17 SNPs instruments with non-zero  $\beta$  while  $\eta_0$  represents the horizontal pleiotropic  
18 effects exhibited by the unselected non-instrumental SNPs with zero  $\beta$ . Controlling for  
19  $\eta_1$  can help mitigate the bias in causal effect estimation induced by horizontal  
20 pleiotropic effects from the instrumental SNPs. While controlling for  $\eta_0$  can reduce  
21 residual error variance in equation (3) and thus help improve the statistical efficiency  
22 of causal effect estimation.

23 To effectively control for the horizontal pleiotropic effects exhibited from both  
24 SNP groups, we specify separate modeling assumptions on  $\eta_0$  and  $\eta_1$ . Specifically,

1 for the selected SNP instruments, we assume that they can exhibit horizontal pleiotropic  
2 effects in two different ways: they can affect the outcome through a common  
3 confounder that is associated with both the exposure and outcome, and they can affect  
4 the outcome through paths independent of the exposure. For the first type of horizontal  
5 pleiotropy, we assume that each selected SNP instrument has a probability of  $\pi_c$  to  
6 induce pleiotropy through the confounder. Following(8), we assume that the  
7 confounder effect on the outcome is  $\rho$  times its effect on the exposure. Consequently,  
8 the effect of the selected SNP instrument acted through the confounder on the outcome  
9 becomes  $\rho\beta_j$ , if the SNP effect on the exposure is  $\beta_j$ . Thus, our assumption on  $\eta_{1j}^c$ ,  
10 which represents the first type of horizontal pleiotropy as a part of  $\boldsymbol{\eta}_1$  for the  $j$ -th SNP,  
11 is  $\eta_{1j}^c|\beta_j \neq 0 \sim \pi_c I(\eta_{1j} = \rho\beta_j) + (1 - \pi_c)\delta_0$ , where  $I(\cdot)$  is an indicator function that  
12 sets the horizontal pleiotropic effect to be  $\rho\beta_j$ . For the second type of horizontal  
13 pleiotropy, we assume that each selected SNP instrument has a probability of  $\pi_1$  to  
14 exhibit a horizontal pleiotropic effect on the outcome directly, bypassing the exposure.  
15 We use  $\eta_{1j}^u$  to represent the second type of horizontal pleiotropy as a part of  $\boldsymbol{\eta}_1$  for  
16 the  $j$ -th SNP. Our assumption on  $\eta_{1j}^u$  is thus  $\eta_{1j}^u|\beta_j \neq 0 \sim \pi_1 N(0, \sigma_\eta^2) + (1 - \pi_1)\delta_0$ ,  
17 where the variance  $\sigma_\eta^2$  determines the strength of the horizontal pleiotropic effect.  
18 Note that the first type of horizontal pleiotropic effects are correlated with the  
19 instrumental effects on the exposure due to the confounder, while the second type of  
20 horizontal pleiotropic effects are uncorrelated with the instrumental effects on the  
21 exposure. The total horizontal pleiotropy is the summation of the two, with  $\eta_{1j} =$   
22  $\eta_{1j}^c + \eta_{1j}^u$ . Certainly, because  $\boldsymbol{\eta}_1$  are the horizontal pleiotropic effects for the selected  
23 SNP instruments, we have  $\eta_{1j} = 0$  if  $\beta_j = 0$ . For the unselected non-instrumental  
24 SNPs with a zero  $\beta_j$ , we assume that  $\eta_{0j}|\beta_j = 0 \sim \pi_0 N(0, \sigma_\eta^2) + (1 - \pi_0)\delta_0$ . That is,

1 with probability  $\pi_0$ , the non-instrumental SNPs display horizontal pleiotropic effects  
2 characterized by the same variance parameter  $\sigma_\eta^2$ . We use the same variance parameter  
3  $\sigma_\eta^2$  for modeling the uncorrelated horizontal pleiotropic effects from both instrumental  
4 and non-instrumental SNPs because we often do not have enough number of SNPs to  
5 estimate two separate parameters accurately. Since  $\boldsymbol{\eta}_0$  are the horizontal pleiotropic  
6 effects for the non-instruments, we also have  $\eta_{0j} = 0$  if  $\beta_j \neq 0$ .

7 The above parameterization of the horizontal pleiotropic effects is based on the  
8 selection of SNP instruments. An equivalent and alternative parametrization of the  
9 horizontal pleiotropic effects is to partition them into a correlated horizontal pleiotropic  
10 component  $\boldsymbol{\eta}_c$  and an uncorrelated horizontal pleiotropic component  $\boldsymbol{\eta}_u$ . Specifically,  
11 the correlated horizontal pleiotropy occurs only for the selected SNP instruments with  
12  $\eta_{cj}|\beta_j \neq 0 \sim \pi_c I(\eta_{1j} = \rho\beta_j) + (1 - \pi_c)\delta_0$  and  $\eta_{cj} = 0$  if  $\beta_j = 0$ . The uncorrelated  
13 horizontal pleiotropy, on the other hand, occurs for both instrumental and non-  
14 instrumental SNPs with  $\eta_{uj}|\beta_j \neq 0 \sim \pi_1 N(0, \sigma_\eta^2) + (1 - \pi_1)\delta_0$  and  $\eta_{uj}|\beta_j =$   
15  $0 \sim \pi_0 N(0, \sigma_\eta^2) + (1 - \pi_0)\delta_0$ . In other words,  $\eta_{cj} = \eta_{1j}^c$  and  $\eta_{uj} = \eta_{1j}^u + \eta_{0j}$ .

16 Overall, the SNP effects on the outcome in our model are exhibited through three  
17 different paths: via the exposure on outcome causal effect  $\alpha$ ; via the correlated  
18 horizontal pleiotropic effects mediated by an unobserved confounder; and via the  
19 uncorrelated horizontal pleiotropic effects. SNPs in the model can exhibit none, one, or  
20 multiple types of these effects. Note that the SNP effects on the outcome through the  
21 causal effect and through the correlated horizontal pleiotropy are not distinguishable  
22 from each other unless we make further modeling assumptions. Here, following(8), we  
23 assume  $\pi_c$  to be small. Thus, among the selected SNP instruments with non-zero  
24 effects on the exposure, only a fraction of them exhibit correlated horizontal pleiotropic  
25 effects on the outcome (details in [Supplementary Text](#)).

1 Our key parameter of interest is the causal effect  $\alpha$ . The causal interpretation of  $\alpha$   
2 in a standard MR model requires the selected SNP instruments to satisfy three  
3 conditions: (i) instruments are associated with the exposure (relevance condition); (ii)  
4 instruments are not associated with any other confounder that may be associated with  
5 both exposure and outcome (independence condition); (iii) instruments only influence  
6 the outcome through the path of exposure (exclusion restriction condition). Our  
7 modeling assumption on  $\beta$  allows us to select SNPs to satisfy the relevance condition.  
8 Our modeling assumptions on  $\eta_0$  and  $\eta_1$  allow us to explicitly model the violation  
9 of the independence and exclusion restriction conditions. Therefore, our model  
10 effectively replaces the general conditions (ii) and (iii) with specific modeling  
11 assumptions on  $\beta$ ,  $\eta_0$  and  $\eta_1$ . In addition, through explicit modeling of the  
12 correlation between the instrument-exposure effects and instrument-outcome effects  
13 through  $\rho$ , our model no longer requires the InSIDE assumption, which is sometimes  
14 referred to as the weak exclusion restriction condition(3). Consequently, the causal  
15 effect interpretation of  $\alpha$  in our model only depends on the explicit assumptions made  
16 in the model.

17 We are interested in estimating the causal effect  $\alpha$  and testing the null hypothesis  
18  $H_0: \alpha = 0$ . Performing inference on  $\alpha$ , however, is computationally challenging, as the  
19 likelihood defined based on the above modeling assumptions is in a complicated form  
20 and involves integrations that cannot be obtained analytically. Here, we develop an  
21 approximate inference algorithm under the maximum likelihood framework to perform  
22 numerical integration of the likelihood and obtain an approximate  $p$ -value for testing  
23  $\alpha$ . Our algorithm is based on the observation that the likelihood function of  $\alpha$  can be  
24 expressed as a ratio between the posterior and the prior. Because the posterior of  $\alpha$  is  
25 asymptotically normally distributed(45, 46), we can use Gibbs sampling to obtain



1 posterior samples of  $\alpha$  and use the sample mean and sample standard deviation to  
2 summarize this posterior distribution. In addition, we can also specify a normal prior  
3 on  $\alpha$  and obtain the prior mean and standard deviation. Because the likelihood of  $\alpha$   
4 is expressed as the posterior divided by the prior and is itself asymptotically normally  
5 distributed(45, 46), we can rely on the method of moments to obtain the approximate  
6 maximum likelihood estimate  $\hat{\alpha}$  and its standard error  $se(\hat{\alpha})$  based on the mean and  
7 standard deviation from both the posterior and the prior. Afterwards, we can construct  
8 an approximate Wald test statistic and obtain a  $p$ -value for hypothesis testing. Details  
9 of the algorithm is provided in the [Supplementary Text](#). Note that, while our algorithm  
10 relies on Gibbs sampling, we do not perform a Bayesian analysis; rather, we treat the  
11 Gibbs sampling as a convenient and accurate numerical approximation tool to obtain  
12 the marginal likelihood of  $\alpha$ , which is otherwise infeasible or inaccurate to obtain  
13 under various frequentist approaches.

14 We refer to our model and algorithm together as the two-sample Mendelian  
15 Randomization with Automated Instrument Determination (MRAID). The automated  
16 instrument determination part highlights the desirable feature of our model in  
17 automatically selecting instrumental variables from a set of candidate ones that are in  
18 potentially high LD with each other. Compared with existing two-sample MR  
19 approaches, MRAID relies on a likelihood inference framework, is capable of modeling  
20 correlated instruments, performs automated instrument selection, controls for both  
21 correlated and uncorrelated horizontal pleiotropy, and is computationally scalable.  
22 MRAID is implemented in an R package, freely available at  
23 [www.xzlab.org/software.html](http://www.xzlab.org/software.html).

24

25 **MRAID for summary statistics**

1 While we have described MRAID using individual-level data, MRAID can be extended  
2 to make use of only summary statistics. Details for the summary statistics version of  
3 MRAID are provided in the [Supplementary Text](#). Briefly, the summary statistics  
4 version of MRAID requires two types of input: the SNP marginal effect size estimates  
5 on the exposure and outcome; and the SNP correlation matrices in the exposure and  
6 outcome GWASs. Both input types are obtained based on standardized genotype data  
7 where the genotypes for each SNP have been standardized to have zero mean and unit  
8 standard deviation. Here, we denote the  $p$ -vector of the SNP marginal effect size  
9 estimates on the exposure as  $\hat{\boldsymbol{\beta}}_x$  and the corresponding vector of marginal effect size  
10 estimates on the outcome as  $\hat{\boldsymbol{\beta}}_y$ . We denote the  $p$  by  $p$  SNP correlation matrix in the  
11 exposure GWAS as  $\Sigma_1$  and the corresponding matrix in the outcome GWAS as  $\Sigma_2$ .  
12 Both  $\Sigma_1$  and  $\Sigma_2$  are positive semi-definite and can be estimated from the same LD  
13 reference panel (e.g. individuals with the same ancestry in the 1,000 Genomes Project).  
14 The MRAID model for summary statistics can be constructed based on the following  
15 two equations

$$16 \quad \hat{\boldsymbol{\beta}}_x = \Sigma_1 \boldsymbol{\beta} + \mathbf{e}_x, \quad (4)$$

$$17 \quad \hat{\boldsymbol{\beta}}_y = \alpha \Sigma_2 \boldsymbol{\beta} + \Sigma_2 \boldsymbol{\eta}_0 + \Sigma_2 \boldsymbol{\eta}_1 + \mathbf{e}_y, \quad (5)$$

18 where  $\mathbf{e}_x$  is a  $p$ -vector of residual error that follows a multivariate normal distribution  
19  $N(0, \Sigma_1 \sigma_x^2 / (n_1 - 1))$ ; and  $\mathbf{e}_y$  is a  $p$ -vector of residual error that follows another a  
20 multivariate normal distribution  $N(0, \Sigma_2 \sigma_y^2 / (n_2 - 1))$ . A similar approximate  
21 inference algorithm under the maximum likelihood framework is developed for the  
22 summary version of MRAID.

23

## 24 **Simulations**

1 We performed realistic simulations to evaluate the performance of MRAID and  
2 compared it with six existing MR methods. For simulations, we randomly selected  
3 60,000 individuals from UK Biobank(19). We split these individuals randomly into two  
4 equal-sized sets: one set with 30,000 individuals to serve as the exposure GWAS and  
5 another set with the remaining 30,000 individuals to serve as the outcome GWAS. For  
6 these individuals, we obtained their genotypes from 649,695 SNPs on chromosome 1  
7 that are overlapped with the GERA study we used before(13), standardized each SNP  
8 to have mean zero and unit standard deviation, and used the standardized genotypes to  
9 simulate the exposure and outcome. Specifically, in the exposure GWAS, we randomly  
10 selected  $K$  SNPs ( $K = 100$  or  $1,000$ ) to have non-zero effects on the exposure. We  
11 denoted the genotype matrix of the  $K$  SNPs as  $\tilde{\mathbf{Z}}_x$ . We simulated the  $K$  SNP effect sizes  
12 on the exposure ( $\boldsymbol{\beta}$ ) from a normal distribution  $N(0, PVE_{\tilde{\mathbf{Z}}_x}/K)$ , where the  
13 scalar  $PVE_{\tilde{\mathbf{Z}}_x}$  represents the proportion of variance in the exposure variable explained  
14 by these genetic effects. We summed the genetic effects across all  $K$  SNPs as  $\tilde{\mathbf{Z}}_x\boldsymbol{\beta}$ . In  
15 addition, we simulated the residual errors  $\boldsymbol{\epsilon}_x$  from a normal distribution  $N(0, 1 -$   
16  $PVE_{\tilde{\mathbf{Z}}_x})$ . We then summed the genetic effects and the residual errors to yield the  
17 simulated exposure variable  $\mathbf{x}$ . In the outcome GWAS, we obtained the genotypes for  
18 the same  $K$  SNPs as  $\tilde{\mathbf{Z}}_y$  and used the same  $\boldsymbol{\beta}$  from the exposure GWAS to compute  
19 the genetic component underlying the outcome as  $\tilde{\mathbf{Z}}_y\boldsymbol{\beta}$ . We set the causal effect  $\alpha$  to  
20 be  $\alpha = \sqrt{PVE_{\alpha}/PVE_{\tilde{\mathbf{Z}}_x}}$ , so that the proportion of variance in the outcome variable  
21 explained by the causal effect term ( $\tilde{\mathbf{Z}}_y\boldsymbol{\beta}\alpha$ ) is  $PVE_{\alpha}$ . We randomly obtained  
22  $\pi_c K$  SNPs (rounded to an integer) from the  $K$  SNPs to exhibit correlated pleiotropy.

1 We simulated the correlated pleiotropic effect sizes to be  $\rho\boldsymbol{\beta}$  and set  $\rho$  so that the  
2 proportion of variance in the outcome variable explained by correlated pleiotropy is  
3  $PVE_c$ . In addition, we randomly obtained  $\pi_1 K$  SNPs (again rounded to an integer) from  
4 the  $K$  SNPs and randomly obtained  $100 - \pi_1 K$  SNPs from the remaining non-causal  
5 SNPs to exhibit uncorrelated pleiotropy, so that a total of 100 SNPs displayed  
6 uncorrelated pleiotropy. We simulated the uncorrelated horizontal pleiotropic effects  
7 for these 100 SNPs from a normal distribution and scaled them so that the proportion  
8 of phenotypic variance in the outcome explained by uncorrelated pleiotropy is  $PVE_u$ .  
9 We simulated the residual errors  $\boldsymbol{\epsilon}_y$  from a normal distribution  $N(0, 1 - PVE_\alpha -$   
10  $PVE_c - PVE_u)$ . We summed the causal effect term, correlated and uncorrelated  
11 horizontal pleiotropic effects, and the residual errors to yield the simulated outcome  $\mathbf{y}$ .

12 We treated the causal SNPs as unknown and followed standard MR procedure to  
13 select SNPs to serve as the instrumental variables. To do so, we used the linear  
14 regression model implemented in GEMMA(47) to perform association analysis in the  
15 exposure GWAS and selected SNPs with a  $p$ -value below  $5 \times 10^{-8}$  as the candidate  
16 instrumental variables for analysis. For the selected SNPs, we obtained their effect size  
17 estimates, standard errors, and  $Z$  scores to serve as the summary statistics input. We  
18 also denoted the standardized genotype matrices for the selected SNPs in the exposure  
19 and outcome GWASs as  $\mathbf{Z}_x$  and  $\mathbf{Z}_y$ , respectively. Based on the genotype matrices,  
20 we obtained the SNP correlation matrices as  $\boldsymbol{\Sigma}_1 = \frac{\mathbf{Z}_x^T \mathbf{Z}_x}{n_1 - 1}$  and  $\boldsymbol{\Sigma}_2 = \frac{\mathbf{Z}_y^T \mathbf{Z}_y}{n_2 - 1}$  to serve as  
21 input for MR model fitting.

1 In the simulations, we first examined a baseline simulation setting where we set  
2  $PVE_{\tilde{z}_x} = 10\%$ ,  $PVE_{\alpha} = 0$ ,  $K = 100$ ,  $\pi_c = 0$ ,  $PVE_u = 0$ ,  $PVE_c = 0$ . On top of the  
3 baseline setting, we varied one parameter at a time to examine the influence of various  
4 parameters on method performance. For  $PVE_{\tilde{z}_x}$ , we set it to be either 5% or 10%. For  
5  $\beta$ , in addition to simulating it from a normal distribution, we also simulated them from  
6 the Bayesian sparse linear mixed model (BSLMM) distribution(38). Specifically, we  
7 randomly selected either 1% or 10% of the  $K$  SNPs to have large effects and these large-  
8 effect SNPs explain 20% of  $PVE_{\tilde{z}_x}$ . We set the remaining SNPs to have small effects  
9 to explain the remaining  $PVE_{\tilde{z}_x}$ . For  $K$ , we set it to be either 100 or 1,000. For  $PVE_{\alpha}$ ,  
10 we set it to be zero in the null simulations and examined different values in the  
11 alternative simulations. In the alternative simulations, we set  $PVE_{\alpha}$  to be 0.05%, 0.15%  
12 or 0.25% when  $K=100$  and set it to be 0.5%, 1.5% and 2.5% when  $K=1,000$  to  
13 ensure sufficient power. For the uncorrelated horizontal pleiotropic effects, we set  
14  $PVE_u$  to be either 0, 2.5% or 5%. Under the null ( $PVE_{\alpha} = 0$ ) in the absence of  
15 uncorrelated horizontal pleiotropy ( $PVE_u = 0$ ), we set  $K$  to be 100 or 1,000. In the  
16 presence of uncorrelated horizontal pleiotropy, we set  $K$  to be 100 and set  $\pi_1$  to be  
17 either 0, 10%, 20%, or 30%. We also simulated the correlated pleiotropy effects and set  
18  $\pi_c$  to be either 5% or 10%, with  $\rho$  being  $\sqrt{0.02}$  or  $\sqrt{0.05}$  following the previous  
19 literature(8).

20 For null simulations, we performed 1,000 simulation replicates in each scenario to  
21 examine type I error control. For power evaluation, we performed 100 alternative  
22 simulations along with 900 null simulations, with which we computed power based on

1 an FDR of 0.05. We then repeated such analysis five times and report the average power  
2 across these replicates. Note that we computed power based on FDR instead of a  
3 nominal  $p$ -value threshold to allow for fair comparison across methods, as the same  $p$ -  
4 value from different methods may correspond to different type I errors.

5

## 6 **Real Data Applications**

7 We applied MRAID and other MR methods to detect causal associations between 38  
8 lifestyle risk factors and 11 CVD-related traits in the UK Biobank. The UK Biobank  
9 data consists of 487,298 individuals and 92,693,895 imputed SNPs(19). We followed  
10 the same sample QC procedure in Neale lab  
11 ([https://github.com/Nealelab/UK\\_Biobank\\_GWAS/tree/master/imputed-v2-gwas](https://github.com/Nealelab/UK_Biobank_GWAS/tree/master/imputed-v2-gwas)) to  
12 retain a total of 337,129 individuals of European ancestry for analysis. We also filtered  
13 out SNPs with an HWE  $p$ -value  $< 10^{-7}$ , a genotype call rate  $< 95\%$ , or an MAF  $< 0.001$   
14 to obtain a total of 13,876,958 SNPs for analysis. For the retained individuals, we  
15 obtained all lifestyle-related quantitative traits and CVD-related traits, removed those  
16 traits with a sample size less than 10,000, and focused on the remaining set of 38  
17 lifestyle traits and 11 CVD-related traits for analysis. The 38 lifestyle traits include 8  
18 physical activity traits, 12 alcohol intake traits, 10 diet traits (e.g. coffee and fruits) and  
19 8 smoking related traits. The 11 CVD-related traits include four pulse wave traits, two  
20 blood pressure traits (SBP and DBP), four lipid traits (LDL, HDL, TC, and TG) and  
21 BMI. Details of these traits are listed in [Table S2](#). Many of these lifestyle risk factors  
22 have been found to be associated with CVD-related traits in observational studies(48-  
23 50), though it remains unclear whether these associations represent causal relationship.  
24 For each trait in turn, we removed the effects of sex and top ten genotype principal

1 components (PCs) to obtain the trait residuals, standardized the residuals to have a mean  
2 of zero and a standard deviation of one, and used these scaled residuals for MR analysis.

3 To mimic the two-sample MR design, we randomly split the 337,129 individuals  
4 into two non-overlap sets: an exposure GWAS set with 168,564 individuals and an  
5 outcome GWAS set with 168,565 individuals. The random data split strategy ensures  
6 sample homogeneity within each study and independence between studies, and was  
7 extensively used in the previous MR literature(6, 51-53). We examined the 38 lifestyle  
8 traits in the exposure GWAS and examined the 11 CVD-related traits in the outcome  
9 GWAS. In both GWASs, we obtained summary statistics for each trait through linear  
10 regression implemented in GEMMA. When lifestyle traits in the exposure GWAS were  
11 treated as the exposure, we selected SNPs with a  $p$ -value below  $5 \times 10^{-8}$  to serve as  
12 the candidate instruments for each exposure trait. Because almost all MR methods  
13 require at least two instrumental SNPs and some methods can become unstable when  
14 the number of instrumental SNPs is too large, we removed exposure traits for which  
15 the number of candidate instruments is either below two or above 10,000. This way, we  
16 removed three traits with less than two candidate instruments and four traits with more  
17 than 10,000 candidate instruments. We paired the remaining 31 exposure lifestyle traits  
18 with 11 outcome CVD-related traits into 341 trait pairs. The mean number of  
19 significantly associated SNPs among the 31 traits is 286. When CVD-related traits in  
20 the outcome GWAS were treated as the exposure, we removed three traits with less  
21 than two candidate instruments, and found that the remaining eight traits have more  
22 than 10,000 candidate instruments. Therefore, for these remaining traits, we used a  
23 more stringent  $p$ -value threshold of  $1 \times 10^{-15}$  to select SNP instruments and analyzed  
24 the resulting 304 trait pairs. The mean number of associated SNPs among the eight  
25 CVD-related traits is 2,318. In total, we analyzed 645 trait pairs.

1

## 2 **Compared Methods**

3 We compared the performance of MRAID with six existing methods that include the  
4 followings. (1) IVW-R, which is the random effects version of IVW. It obtains the  
5 causal effect estimate through weighting and combining the effect estimates from  
6 individual instruments. It relies on random effects to account for pleiotropy and effect  
7 estimate heterogeneity across instruments(54). (2) Weighted mode, which is a mode  
8 version of IVW. It obtains the causal effect estimate as the mode, instead of the mean,  
9 of the effect estimates obtained from individual instruments(55). (3) Robust, which is  
10 a robust version of IVW. It uses the MM-estimation procedure consisting of an initial  
11 S-estimate followed by an M-estimate(56) that is further combined with Tukey's bi-  
12 weight loss function(57). We fitted methods (1)-(3) using R package  
13 'MendelianRandomization' with default settings. (4) RAPS, which is the MR Adjusted  
14 Profile Score method. It incorporates random effects and robust loss functions into the  
15 profile score to account for systematic and idiosyncratic pleiotropy(6). We fitted RAPS  
16 using R package 'mr.raps'; (5) MRMix, which relies on a mixture model to account for  
17 horizontal pleiotropic effects and their correlation with instrumental effect sizes(7). We  
18 fitted MRMix using R package 'MRMix'. (6) CAUSE, which identifies instrumental  
19 effect size patterns that are consistent with causal effects while accounting for  
20 correlated pleiotropy(8). We fitted CAUSE using R package 'cause'. We compared  
21 MRAID with the above six methods because CAUSE is one of the most recently  
22 developed methods; IVW-R, Robust and RAPS all have been shown to have superior  
23 performance when the InSIDE assumption is satisfied; while MRMix and Weighted  
24 mode perform well even the InSIDE assumption is violated(8, 20). In both simulations  
25 and real data applications, we first obtained SNPs that achieve genome-wide



1 significance level ( $p < 5 \times 10^{-8}$ ) to serve as a candidate set of instrumental SNPs. We  
2 directly use this candidate set of instrumental SNPs for MRAID. Because all other MR  
3 methods require independent instrumental SNPs, we performed LD clumping on the  
4 candidate set of instrumental SNPs to select independent ones for analysis. LD  
5 clumping is performed using PLINK, where we set the LD  $r^2$  parameter to be 0.001.  
6 CAUSE also requires estimating some nuisance parameters in the model by using a  
7 random set of SNPs across the genome, and we did so by randomly selecting 100,000  
8 SNPs following(8). Finally, we explored an oracle approach in the power simulations  
9 where we knew the actual set of instrumental SNPs that affect the exposure variable. In  
10 the oracle approach, we obtained the actual set of instrumental SNPs, selected among  
11 them the independent ones via pruning, and used the selected set of SNPs to serve as  
12 instruments using the IVW-R method. The compared methods and their corresponding  
13 software are listed in [Table S3](#).  
14

## 1   **References**

- 2   1.    S. Burgess, D. S. Small, S. G. Thompson, A review of instrumental variable  
3        estimators for Mendelian randomization. *Stat. Methods Med. Res* **26**, 2333-2355  
4        (2017).
- 5   2.    S. Burgess, A. Butterworth, S. G. Thompson, Mendelian randomization analysis  
6        with multiple genetic variants using summarized data. *Genetic epidemiology* **37**,  
7        658-665 (2013).
- 8   3.    J. Bowden, G. D. Smith, S. Burgess, Mendelian randomization with invalid  
9        instruments: effect estimation and bias detection through Egger regression. *Int.*  
10       *J. Epidemiol.* **44**, 512-525 (2015).
- 11 4.    J. Bowden, G. Davey Smith, P. C. Haycock, S. Burgess, Consistent Estimation  
12        in Mendelian Randomization with Some Invalid Instruments Using a Weighted  
13        Median Estimator. *Genetic epidemiology* **40**, 304-314 (2016).
- 14 5.    J. Zhao, J. Ming, X. Hu, G. Chen, J. Liu, C. Yang, Bayesian weighted  
15        Mendelian randomization for causal inference based on summary statistics.  
16        *Bioinformatics* **36**, 1501-1508 (2020).
- 17 6.    Q. Zhao, J. Wang, G. Hemani, J. Bowden, D. S. J. A. o. S. Small, Statistical  
18        inference in two-sample summary-data Mendelian randomization using robust  
19        adjusted profile score. *Ann. Stat.* **48**, 1742-1769 (2020).
- 20 7.    G. Qi, N. Chatterjee, Mendelian randomization analysis using mixture models  
21        for robust and efficient estimation of causal effects. *Nat. Commun.* **10**, 1941  
22        (2019).
- 23 8.    J. Morrison, N. Knoblauch, J. H. Marcus, M. Stephens, X. J. N. G. He,  
24        Mendelian randomization accounting for correlated and uncorrelated

- 1 pleiotropic effects using genome-wide summary statistics. *Nat. Genet.*, 1-7  
2 (2020).
- 3 9. S. Burgess, F. Dudbridge, S. G. Thompson, Combining information on multiple  
4 instrumental variables in Mendelian randomization: comparison of allele score  
5 and summarized data methods. *Stat. Med.* **35**, 1880-1906 (2016).
- 6 10. S. Burgess, S. G. Thompson, Bias in causal estimates from Mendelian  
7 randomization studies with weak instruments. *Stat. Med.* **30**, 1312-1323 (2011).
- 8 11. A. Gusev, A. Ko, H. Shi, G. Bhatia, W. Chung, B. W. Penninx, R. Jansen, E. J.  
9 de Geus, D. I. Boomsma, F. A. Wright, Integrative approaches for large-scale  
10 transcriptome-wide association studies. *Nat. Genet.* **48**, 245-252 (2016).
- 11 12. P. Zeng, X. Zhou, Non-parametric genetic prediction of complex traits with  
12 latent Dirichlet process regression models. *Nat. Commun.* **8**, 456 (2017).
- 13 13. Z. Yuan, H. Zhu, P. Zeng, S. Yang, S. Sun, C. Yang, J. Liu, X. Zhou, Testing  
14 and controlling for horizontal pleiotropy with probabilistic Mendelian  
15 randomization in transcriptome-wide association studies. *Nat. Commun.* **11**,  
16 3861 (2020).
- 17 14. L. Liu, P. Zeng, F. Xue, Z. Yuan, X. Zhou, Multi-trait transcriptome-wide  
18 association studies with probabilistic Mendelian randomization. *Am. J. Hum.*  
19 *Genet.* **108**, 240-256 (2021).
- 20 15. M. Verbanck, C. Y. Chen, B. Neale, R. Do, Detection of widespread horizontal  
21 pleiotropy in causal relationships inferred from Mendelian randomization  
22 between complex traits and diseases. *Nat. Genet.* **50**, 693-698 (2018).
- 23 16. Z. Zhu, Z. Zheng, F. Zhang, Y. Wu, M. Trzaskowski, R. Maier, M. R. Robinson,  
24 J. J. McGrath, P. M. Visscher, N. R. Wray, J. Yang, Causal associations between

- 1 risk factors and common diseases inferred from GWAS summary data. *Nat.*  
2 *Commun.* **9**, 224 (2018).
- 3 17. P. Zeng, T. Wang, J. Zheng, X. Zhou, Causal association of type 2 diabetes with  
4 amyotrophic lateral sclerosis: new evidence from Mendelian randomization  
5 using GWAS summary statistics. *BMC Med.* **17**, 225 (2019).
- 6 18. P. Zeng, X. Zhou, Causal effects of blood lipids on amyotrophic lateral sclerosis:  
7 a Mendelian randomization study. *Hum. Mol. Genet.* **28**, 688-697 (2019).
- 8 19. C. Bycroft, C. Freeman, D. Petkova, G. Band, L. T. Elliott, K. Sharp, A. Motyer,  
9 D. Vukcevic, O. Delaneau, J. O'Connell, The UK Biobank resource with deep  
10 phenotyping and genomic data. *Nature* **562**, 203-209 (2018).
- 11 20. G. Qi, N. Chatterjee, A comprehensive evaluation of methods for Mendelian  
12 randomization using realistic simulations and an analysis of 38 biomarkers for  
13 risk of type 2 diabetes. *Int. J. Epidemiol.*, (2021).
- 14 21. D. Mozaffarian, P. W. Wilson, W. B. Kannel, Beyond established and novel  
15 risk factors: lifestyle risk factors for cardiovascular disease. *Circulation* **117**,  
16 3031-3038 (2008).
- 17 22. B. H. Brummett, M. A. Babyak, I. C. Siegler, M. Shanahan, K. M. Harris, G. H.  
18 Elder, R. B. Williams, Systolic blood pressure, socioeconomic status, and  
19 biobehavioral risk factors in a nationally representative US young adult sample.  
20 *Hypertension* **58**, 161-166 (2011).
- 21 23. A. R. Barker, L. Gracia-Marco, J. R. Ruiz, M. J. Castillo, R. Aparicio-Ugarriza,  
22 M. Gonzalez-Gross, A. Kafatos, O. Androutsos, A. Polito, D. Molnar, K.  
23 Widhalm, L. A. Moreno, Physical activity, sedentary time, TV viewing,  
24 physical fitness and cardiovascular disease risk in adolescents: The HELENA  
25 study. *Int. J. Cardiol.* **254**, 303-309 (2018).

- 1 24. N. T. Hadgraft, E. Winkler, R. E. Climie, M. S. Grace, L. Romero, N. Owen, D.  
2 Dunstan, G. Healy, P. C. Dempsey, Effects of sedentary behaviour interventions  
3 on biomarkers of cardiometabolic risk in adults: systematic review with meta-  
4 analyses. *Br. J. Sports Med.* **55**, 144-154 (2021).
- 5 25. S. Dare, D. F. Mackay, J. P. Pell, Relationship between smoking and obesity: a  
6 cross-sectional study of 499,504 middle-aged adults in the UK general  
7 population. *PLOS ONE* **10**, e0123579 (2015).
- 8 26. Z. Yuan, J. Ji, T. Zhang, Y. Liu, X. Zhang, W. Chen, F. Xue, A novel chi-square  
9 statistic for detecting group differences between pathways in systems  
10 epidemiology. *Stat. Med.* **35**, 5512-5524 (2016).
- 11 27. U. C. Winslow, L. Rode, B. G. Nordestgaard, High tobacco consumption lowers  
12 body weight: a Mendelian randomization study of the Copenhagen General  
13 Population Study. *Int. J. Epidemiol.* **44**, 540-550 (2015).
- 14 28. A. Hofstetter, Y. Schutz, E. Jequier, J. Wahren, Increased 24-hour energy  
15 expenditure in cigarette smokers. *N. Engl. J. Med.* **314**, 79-82 (1986).
- 16 29. R. J. Moffatt, S. G. Owens, Cessation from cigarette smoking: changes in body  
17 weight, body composition, resting metabolism, and energy consumption.  
18 *Metabolism* **40**, 465-470 (1991).
- 19 30. C. M. Ferrara, M. Kumar, B. Nicklas, S. McCrone, A. P. Goldberg, Weight gain  
20 and adipose tissue metabolism after smoking cessation in women. *Int. J. Obes.*  
21 **25**, 1322-1326 (2001).
- 22 31. Y. H. Jo, D. A. Talmage, L. W. Role, Nicotinic receptor-mediated effects on  
23 appetite and food intake. *J. Neurosci.* **53**, 618-632 (2002).
- 24 32. Y. S. Mineur, A. Abizaid, Y. Rao, R. Salas, R. J. DiLeone, D. Gundisch, S.  
25 Diano, M. De Biasi, T. L. Horvath, X. B. Gao, M. R. Picciotto, Nicotine

- 1 decreases food intake through activation of POMC neurons. *Science* **332**, 1330-  
2 1332 (2011).
- 3 33. D. B. Rosoff, G. Davey Smith, N. Mehta, T. K. Clarke, F. W. Lohoff, Evaluating  
4 the relationship between alcohol consumption, tobacco use, and cardiovascular  
5 disease: A multivariable Mendelian randomization study. *PLOS Med.* **17**,  
6 e1003410 (2020).
- 7 34. B. M. He, S. P. Zhao, Z. Y. Peng, Effects of cigarette smoking on HDL quantity  
8 and function: implications for atherosclerosis. *J. Cell. Biochem.* **114**, 2431-2436  
9 (2013).
- 10 35. A. D. Gepner, M. E. Piper, H. M. Johnson, M. C. Fiore, T. B. Baker, J. H. Stein,  
11 Effects of smoking and smoking cessation on lipids and lipoproteins: outcomes  
12 from a randomized clinical trial. *Am. Heart J.* **161**, 145-151 (2011).
- 13 36. A. Linneberg, R. K. Jacobsen, T. Skaaby, A. E. Taylor, M. E. Fluharty, J. L.  
14 Jeppesen, J. H. Bjorngaard, B. O. Asvold, M. E. Gabrielsen, A. Campbell, R. E.  
15 Marioni, M. Kumari, P. Marques-Vidal, M. Kaakinen, A. Cavadino, I. Postmus,  
16 T. S. Ahluwalia, S. G. Wannamethee, J. Lahti, K. Raikonen, A. Palotie, A.  
17 Wong, C. Dalgard, I. Ford, Y. Ben-Shlomo, L. Christiansen, K. O. Kyvik, D.  
18 Kuh, J. G. Eriksson, P. H. Whincup, H. Mbarek, E. J. de Geus, J. M. Vink, D.  
19 I. Boomsma, G. D. Smith, D. A. Lawlor, A. Kisiailiou, A. McConnachie, S.  
20 Padmanabhan, J. W. Jukema, C. Power, E. Hypponen, M. Preisig, G. Waeber,  
21 P. Vollenweider, T. Korhonen, T. Laatikainen, V. Salomaa, J. Kaprio, M.  
22 Kivimaki, B. H. Smith, C. Hayward, T. I. Sorensen, B. H. Thuesen, N. Sattar,  
23 R. W. Morris, P. R. Romundstad, M. R. Munafo, M. R. Jarvelin, L. L.  
24 Husemoen, Effect of Smoking on Blood Pressure and Resting Heart Rate: A

- 1 Mendelian Randomization Meta-Analysis in the CARTA Consortium.  
2 *Circulation: Cardiovascular Genetics* **8**, 832-841 (2015).
- 3 37. R. E. Luehrs, D. Zhang, G. L. Pierce, D. R. Jacobs, Jr., R. Kalhan, K. M.  
4 Whitaker, Cigarette Smoking and Longitudinal Associations With Blood  
5 Pressure: The CARDIA Study. *J. Am. Heart Assoc.* **10**, e019566 (2021).
- 6 38. X. Zhou, P. Carbonetto, M. Stephens, Polygenic modeling with bayesian sparse  
7 linear mixed models. *PLoS Genet.* **9**, e1003264 (2013).
- 8 39. T. G. Richardson, E. Sanderson, B. Elsworth, K. Tilling, G. Davey Smith, Use  
9 of genetic variation to separate the effects of early and later life adiposity on  
10 disease risk: mendelian randomisation study. *BMJ* **369**, m1203 (2020).
- 11 40. J. Vaucher, B. J. Keating, A. M. Lasserre, W. Gan, D. M. Lyall, J. Ward, D. J.  
12 Smith, J. P. Pell, N. Sattar, G. Pare, M. V. Holmes, Cannabis use and risk of  
13 schizophrenia: a Mendelian randomization study. *Mol. Psychiatry* **23**, 1287-  
14 1292 (2018).
- 15 41. M. Gormley, T. Dudding, E. Sanderson, R. M. Martin, S. Thomas, J. Tyrrell, A.  
16 R. Ness, P. Brennan, M. Munafò, M. Pring, S. Boccia, A. F. Olshan, B.  
17 Diergaarde, R. J. Hung, G. Liu, G. Davey Smith, R. C. Richmond, A  
18 multivariable Mendelian randomization analysis investigating smoking and  
19 alcohol consumption in oral and oropharyngeal cancer. *Nat. Commun.* **11**, 6071  
20 (2020).
- 21 42. S. Burgess, J. A. Labrecque, Mendelian randomization with a binary exposure  
22 variable: interpretation and presentation of causal estimates. *Eur. J. Epidemiol.*  
23 **33**, 947-952 (2018).
- 24 43. M. Baiocchi, J. Cheng, D. S. Small, Instrumental variable methods for causal  
25 inference. *Stat. Med.* **33**, 2297-2340 (2014).

- 1 44. P. H. Allman, I. Aban, D. M. Long, S. L. Bridges, Jr., V. Srinivasasainagendra,  
2 T. MacKenzie, G. Cutter, H. K. Tiwari, A novel Mendelian randomization  
3 method with binary risk factor and outcome. *Genetic epidemiology*, (2021).
- 4 45. A. J. Lea, J. Tung, X. Zhou, A Flexible, Efficient Binomial Mixed Model for  
5 Identifying Differential DNA Methylation in Bisulfite Sequencing Data. *PLoS*  
6 *Genet.* **11**, e1005650 (2015).
- 7 46. S. Sun, M. Hood, L. Scott, Q. Peng, S. Mukherjee, J. Tung, X. Zhou,  
8 Differential expression analysis for RNAseq using Poisson mixed models.  
9 *Nucleic Acids Res.* **45**, e106 (2017).
- 10 47. X. Zhou, M. Stephens, Genome-wide efficient mixed-model analysis for  
11 association studies. *Nat. Genet.* **44**, 821-824 (2012).
- 12 48. M. J. Stampfer, F. B. Hu, J. E. Manson, E. B. Rimm, W. C. Willett, Primary  
13 prevention of coronary heart disease in women through diet and lifestyle. *N.*  
14 *Engl. J. Med.* **343**, 16-22 (2000).
- 15 49. A. O. Odegaard, W. P. Koh, M. D. Gross, J. M. Yuan, M. A. Pereira, Combined  
16 lifestyle factors and cardiovascular disease mortality in Chinese men and  
17 women: the Singapore Chinese health study. *Circulation* **124**, 2847-2854  
18 (2011).
- 19 50. R. R. Huxley, M. Woodward, Cigarette smoking as a risk factor for coronary  
20 heart disease in women compared with men: a systematic review and meta-  
21 analysis of prospective cohort studies. *Lancet* **378**, 1297-1305 (2011).
- 22 51. E. Mountjoy, N. M. Davies, D. Plotnikov, G. D. Smith, S. Rodriguez, C. E.  
23 Williams, J. A. Guggenheim, D. Atan, Education and myopia: assessing the  
24 direction of causality by mendelian randomisation. *BMJ* **361**, k2022 (2018).



- 1 52. A. Henry, M. Katsoulis, S. Masi, G. Fatemifar, S. Denaxas, D. Acosta, V.  
2 Garfield, C. E. Dale, The relationship between sleep duration, cognition and  
3 dementia: a Mendelian randomization study. *Int. J. Epidemiol.* **48**, 849-860  
4 (2019).
- 5 53. Q. Zhao, J. Wang, W. Spiller, J. Bowden, D. S. J. S. s. Small, Two-sample  
6 instrumental variable analyses using heterogeneous samples. *Stat. Sci.* **34**, 317-  
7 333 (2019).
- 8 54. J. Bowden, M. F. Del Greco, C. Minelli, G. Davey Smith, N. Sheehan, J.  
9 Thompson, A framework for the investigation of pleiotropy in two-sample  
10 summary data Mendelian randomization. *Stat. Med.* **36**, 1783-1802 (2017).
- 11 55. F. P. Hartwig, G. Davey Smith, J. Bowden, Robust inference in summary data  
12 Mendelian randomization via the zero modal pleiotropy assumption. *Int. J.*  
13 *Epidemiol.* **46**, 1985-1998 (2017).
- 14 56. M. Koller, W. A. J. C. S. Stahel, D. Analysis, Sharpening wald-type inference  
15 in robust regression for small samples. *Comput. Stat. Data Anal.* **55**, 2504-2515  
16 (2011).
- 17 57. S. Burgess, J. Bowden, F. Dudbridge, S. G. J. a. p. a. Thompson, Robust  
18 instrumental variable methods using multiple candidate instruments with  
19 application to Mendelian randomization. *arXiv preprint arXiv:1608.02990*,  
20 (2016).
- 21

## 1 **Acknowledgements**

2 **Funding:** ZY was supported by the National Natural Science Foundation of China  
3 (81872712), the Natural Science Foundation of Shandong Province (ZR2019ZD02) and  
4 the Young Scholars Program of Shandong University (2016WLJH23). XZ was  
5 supported by the University of Michigan. This study has been conducted using UK  
6 Biobank resource under Application Number 51470. UK Biobank was established by  
7 the Wellcome Trust medical charity, Medical Research Council, Department of Health,  
8 Scottish Government and the Northwest Regional Development Agency. It also has  
9 funding from the Welsh Assembly Government, British Heart Foundation and Diabetes  
10 UK.

11 **Author contributions:** XZ conceived the idea. XZ and ZY developed the methods. ZY  
12 developed the software tool with assistance from LL. ZY performed simulations and  
13 real data analysis with assistance from LL, PG, RY and FX. XZ and ZY wrote the  
14 manuscript with input from all other authors. All authors reviewed and approved the  
15 final manuscript.

16 **Competing interests:** Authors declare that they have no competing interests.

17 **Data and materials availability:** No data are generated in the present study. The UK  
18 Biobank data is from UK Biobank resource under application number 51470. The  
19 MRAID is implemented in the R package MRAID, freely available on GitHub  
20 (<https://github.com/yuanzhongshang/MRAID>).

21

22

**Table 1 Mean computational time (in minutes) of various two-sample MR methods.**

#SNPs	MRAID	CAUSE	MRMix	IVW-R	Weighted mode	RAPS	Robust
1000	0.31(0.07)	2.63(1.90)	0.12(0.03)	0.0001(0.00001)	0.17(0.04)	0.0004(0.0003)	0.0004(0.0001)
2000	1.57(0.26)	2.99(2.24)	0.13(0.03)	0.0001(0.00001)	0.18(0.03)	0.0004(0.0006)	0.0004(0.0001)
3000	3.91(0.75)	3.66(2.36)	0.14(0.02)	0.0001(0.00002)	0.18(0.03)	0.0004(0.0003)	0.0004(0.0001)
4000	6.82(1.35)	4.24(1.62)	0.15(0.04)	0.0001(0.00003)	0.18(0.04)	0.0004(0.0001)	0.0004(0.0002)
5000	10.80(2.69)	4.92(2.29)	0.18(0.05)	0.0001(0.00004)	0.18(0.04)	0.0004(0.0001)	0.0005(0.0003)

Computation is carried out on a single thread of a Xeon Gold 6138 CPU. The computation time is averaged across 20 replicates, with values inside parentheses denoting the standard deviation. #SNPs denotes the number of instrumental variables included in the model. The computational time for MRAID is based on 1,000 Gibbs sampling iterations with the first 200 as burn-in.

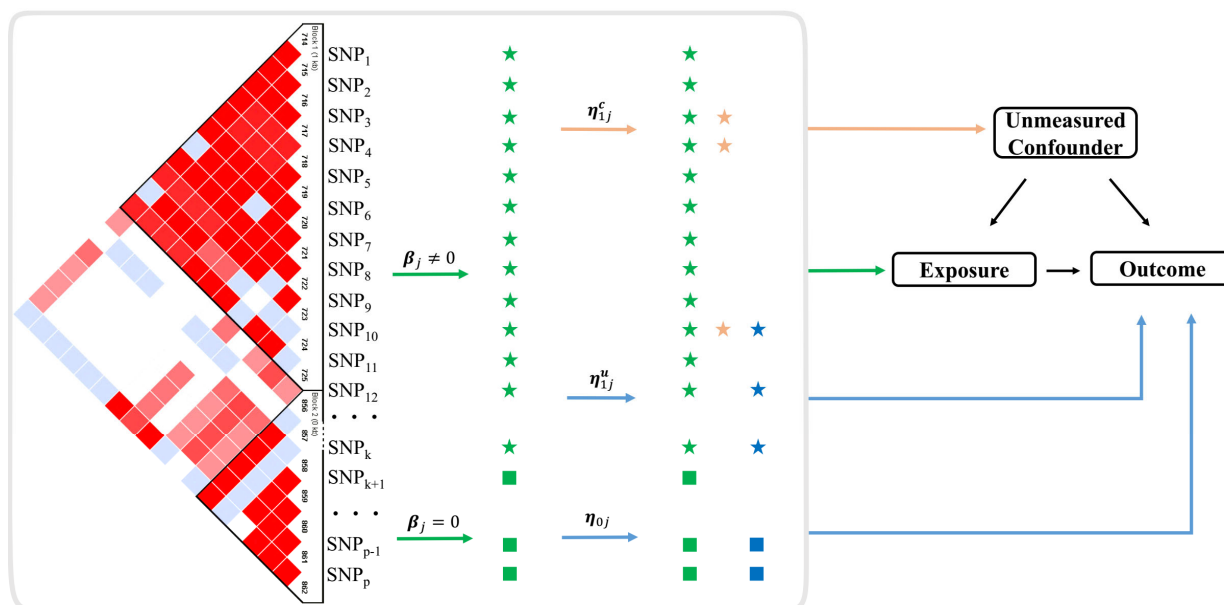


**Fig. 1 Schematic of MR-AID.** MR-AID is a Mendelian randomization method that infers the causal effect of an exposure on an outcome in the presence of unmeasured confounder by using SNPs as instrumental variables. MR-AID first obtains an initial set of candidate SNP instruments that are marginally associated with the exposure ( $SNP_1, \dots, SNP_p$ ) and that are in potential LD with each other (LD plot on left). MR-AID imposes a sparsity assumption on the instrumental effects of the candidate SNPs to select instruments with non-zero effects on the exposure (green stars, selected by a green arrow). Among the selected instruments, MR-AID assumes that a proportion of them display horizontal pleiotropic effects that are uncorrelated with instrumental effects (blue stars, selected by a blue arrow) and that another proportion of them display horizontal pleiotropic effects that are correlated with instrumental effects (orange stars, selected by an orange arrow). Among the non-selected instrument candidates (green squares, selected by a green arrow), MR-AID also assumes that a proportion of them display horizontal pleiotropic effects that are uncorrelated with instrumental effects (blue squares, selected by a blue arrow). Overall, MR-AID models jointly all genome-wide significant SNPs that are in potential LD with each other and performs automated instrument selection among them to identify suitable instruments. MR-AID explicitly accounts for both correlated and uncorrelated horizontal pleiotropy and relies on a likelihood framework for effective and scalable inference.

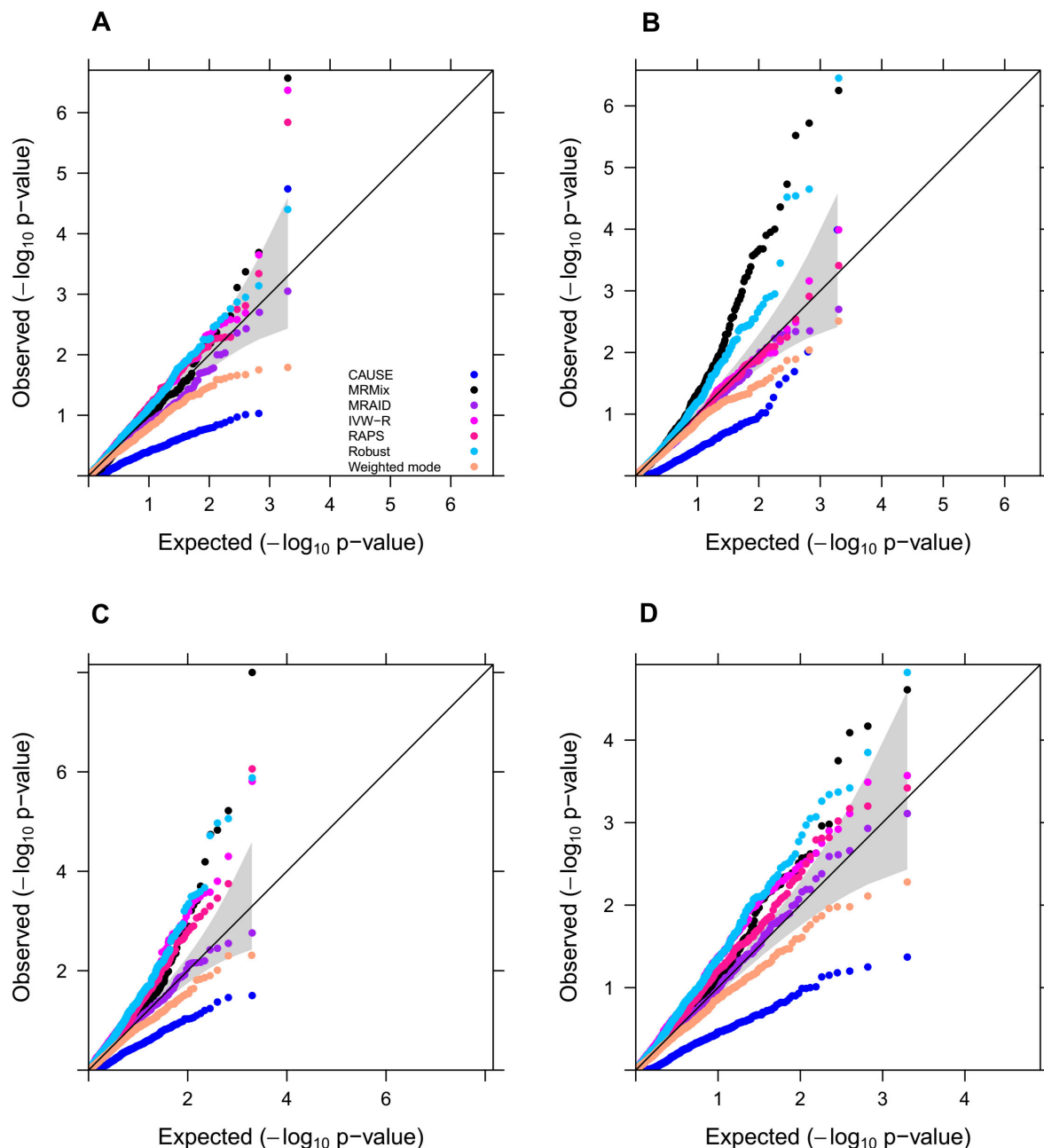


**Fig. 2 Type I error control of different MR methods in simulations.** Type I error is evaluated by quantile-quantile plots of  $-\log_{10}$  p-values from different MR methods on testing the causal effect under the null simulations. Compared methods include CAUSE (blue), MRMix (black), MRAID (purple), IVW-R (magenta), RAPS (deep pink), Robust (deep sky blue), Weighted mode (light salmon). Four null simulation scenarios are examined. **(A)** Null simulations in the absence of both correlated and uncorrelated horizontal pleiotropic effects. We simulated 100 instrumental SNPs with their effect sizes drawing from a normal distribution. **(B)** Null simulations in the absence of both correlated and uncorrelated horizontal pleiotropic effects. We simulated 1,000 instrumental SNPs with their effect sizes drawing from a BSLMM distribution with 1% SNPs having large effects and 99% SNPs having small effects. **(C)** Null simulations in the absence of correlated horizontal pleiotropic effect but in the presence of uncorrelated horizontal pleiotropic effect ( $PVE_u = 5\%$ ). We simulated 100 instrumental SNPs and set the proportion of instrumental SNPs having uncorrelated horizontal pleiotropy to be 20%. **(D)** Null simulations in the presence

of both correlated ( $\pi_c = 5\%$ ,  $\rho = \sqrt{0.05}$ ) and uncorrelated horizontal pleiotropic effects ( $PVE_u = 5\%$ ). We simulated 100 instrumental SNPs and set the proportion of instrumental SNPs having the uncorrelated horizontal pleiotropy effect to be 20%.

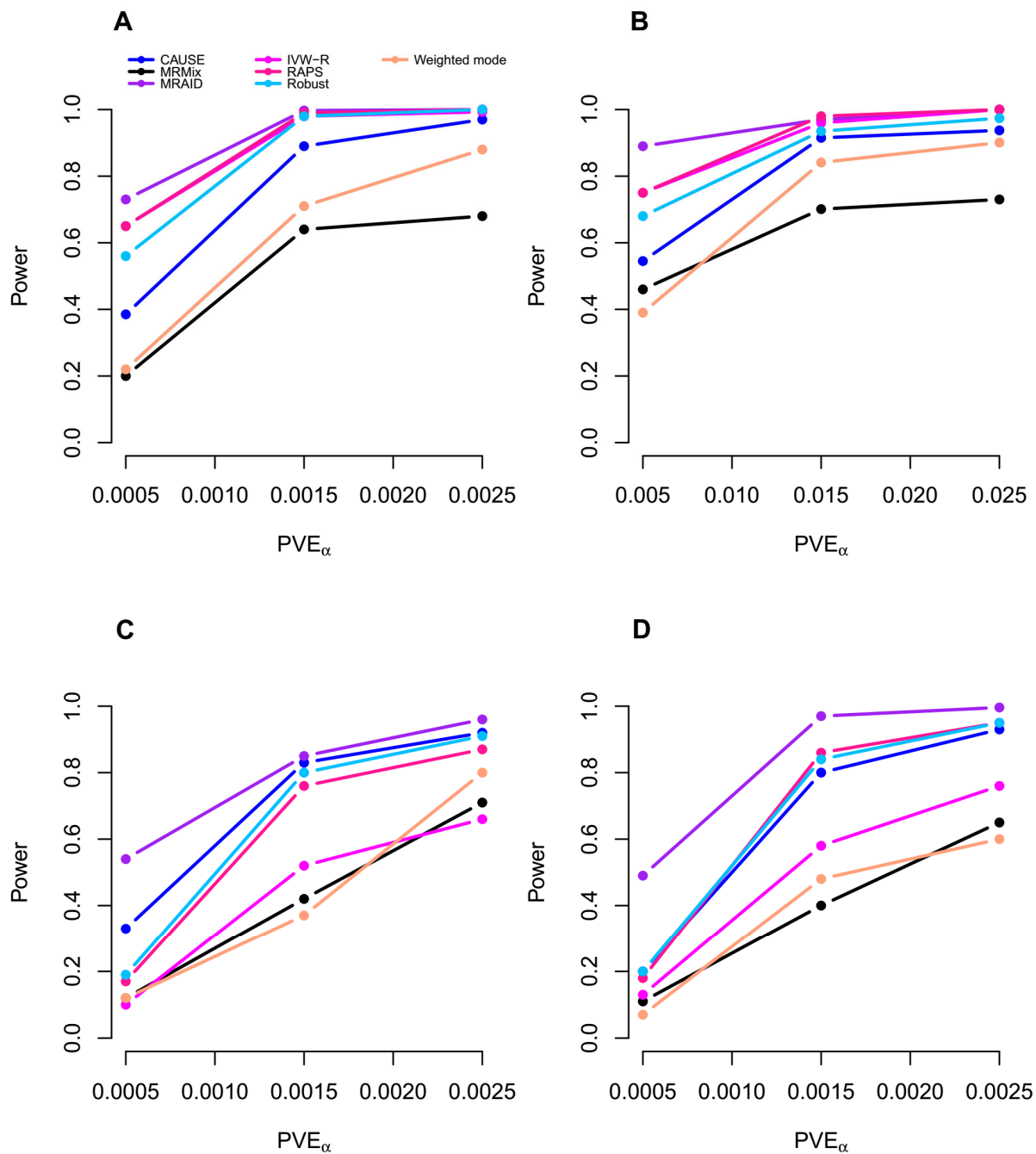


**Fig. 3 Power of different MR methods in simulations.** Power (y-axis) at a false discovery rate of 0.05 to detect the causal effect is plotted against different causal effect size characterized by  $PVE_{\alpha}$  (x-axis). Compared methods include CAUSE (blue), MRMix (black), MRAID (purple), IVW-R (magenta), RAPS (deep pink), Robust (deep sky blue), Weighted mode (light salmon). Four alternative simulation scenarios are examined. (A) Simulations in the absence of both correlated and uncorrelated horizontal pleiotropic effects. We simulated 100 instrumental SNPs with their effects size drawing from a normal distribution. (B) Simulations in the absence of both correlated and uncorrelated horizontal pleiotropic effects. We simulated 1,000 instrumental SNPs with their effects size drawing from a BSLMM distribution with 1% SNPs having large effects and 99% SNPs having small effects. (C) Simulations in the absence of correlated horizontal pleiotropic effect but in the presence of uncorrelated horizontal pleiotropic effect ( $PVE_u = 5\%$ ). We simulated 100 instrumental SNPs and set the proportion of instrumental SNPs having the

uncorrelated horizontal pleiotropy effect to be 30%. **(D)** Simulations in the presence of both correlated ( $\pi_c = 5\%$ ,  $\rho = \sqrt{0.05}$ ) and uncorrelated horizontal pleiotropic effects ( $PVE_u = 5\%$ ). We simulated 100 causal instrumental SNPs and set the proportion of instrumental SNPs having the uncorrelated horizontal pleiotropy effect to be 20%.



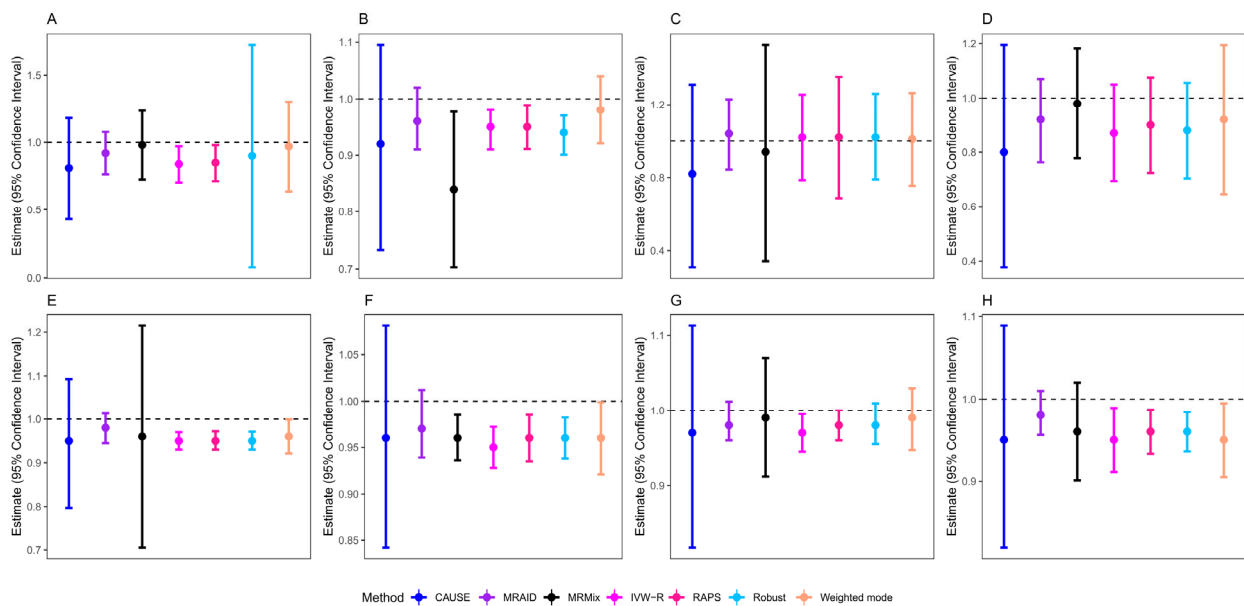


**Fig. 4 Point estimates and 95% confidence intervals from different MR methods in the trait on itself analysis in the real data.** Compared methods include CAUSE (blue), MRMix (black), MRAID (purple), IVW-R (magenta), RAPS (deep pink), Robust (deep sky blue), Weighted mode (light salmon). Analyzed trait pairs include SBP-SBP (A), BMI-BMI (B), DBP-DBP (C), Pulse rate-Pulse rate (D), TC-TC (E), LDL-LDL (F), TG-TG (G), and HDL-HDL (H). The horizontal black dashed line in each panel represents the true causal effect size of  $\alpha=1$ . Both MRAID and CAUSE can produce 95% confidence intervals that cover the true causal effects of all trait pairs, with CAUSE producing much larger confidence intervals than MRAID.

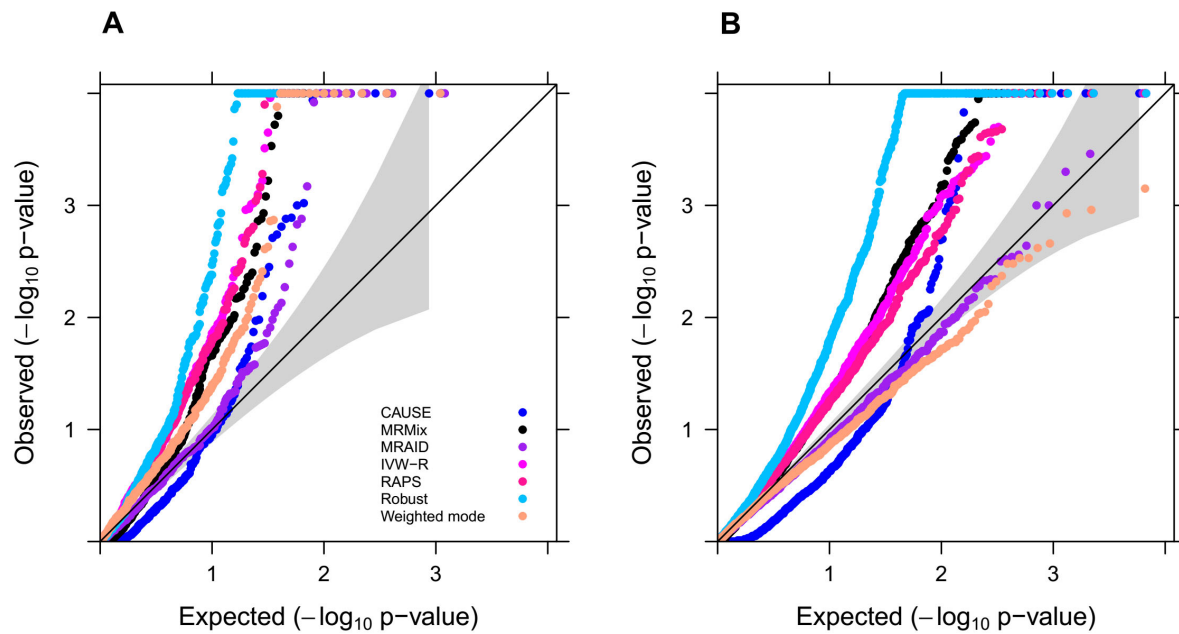


**Fig. 5** Quantile-quantile plot of  $-\log_{10}$  p-values from different MR methods on testing the causal relationship between lifestyle risk factors and CVD-related traits in UK Biobank. Compared methods include CAUSE (blue), MRMix (black), MRAID (purple), IVW-R (magenta), RAPS (deep pink), Robust (deep sky blue), and Weighted mode (light salmon). The results are shown for all 645 analyzed trait pairs (A) and the empirical null where we permuted the outcome ten times in the MR analysis of lifestyle traits on CVD-related traits (B).